CHIN. PHYS. LETT. Vol. 36, No. 8 (2019) 080305 **Express Letter**

Quantum Approach to Fast Protein-Folding Time *

Li-Hua Lu(吕丽花)[1], You-Quan Li(李有泉)[1,2]**

[1]*Zhejiang Province Key Laboratory of Quantum Technology & Device, and Department of Physics, Zhejiang University, Hangzhou 310027*

[2]*Collaborative Innovation Center of Advanced Microstructure, Nanjing University, Nanjing 210008*

(Received 26 July 2019)

In the traditional random-conformational-search model, various hypotheses with a series of meta-stable intermediate states were proposed to resolve the Levinthal paradox in protein-folding time. Here we introduce a quantum strategy to formulate protein folding as a quantum walk on a definite graph, which provides us a general framework without making hypotheses. Evaluating it by the mean of first passage time, we find that the folding time via our quantum approach is much shorter than the one obtained via classical random walks. This idea is expected to evoke more insights for future studies.

PACS: 03.67.Ac, 87.15.hm, 05.40.Fb DOI: 10.1088/0256-307X/36/8/080305

Understanding how proteins fold spontaneously into their native structures is a fascinating and fundamental problem in interdisciplinary fields involving molecular biology, computer science, polymer physics as well as theoretical physics etc. Since Harrington and Schellman found that protein-folding reactions are very fast and often reversible processes,[1] there has been progressively more investigations on protein folding in both aspects of theory and experiment. Levinthal[2] noted early in 1967 that a much larger folding time is inevitable if proteins are folded by sequentially sampling of all possible conformations. Thus the protein was assumed to fold through a series of meta-stable intermediate states and the random conformational search does not occur in the folding process. The questions about what are the energetics of folding and how the denature cause unfolding motivate researchers to think that the protein folding proceeds energetically downhill and loses conformational entropy as it goes. Based on such a hypothesis, the free-energy landscape framework was one way to describe the protein folding,[3–5] where the energy funnel landscape provided a first conjecture of how the folding begins and continues.[6]

As we know, there have been substantial theoretical models with different simplifying assumptions, such as the Ising-like model,[7,8] the foldon-dependent protein folding model,[9] the diffusion-collision model,[10,11] and the nucleation-condensation mechanism.[12,13] Theoretical models are useful for understanding the essentials of the complex self-assembly reaction of protein folding. However, till now they often rely on various hypotheses.[6,14–17] This often brings in certain difficulties in connecting analytical theory to experimental results because some hypotheses can not be easily put into a practical experimental measurement. As it introduces less hypotheses in comparison to those theoretical models, the atomistic simulations[18–20] were used to investigate the protein folding along with nowadays' advances in computer science. Recently, a high-throughput protein design and characterization method was reported to allow one to systematically examine how sequence determines the folding and stability.[21] However, quantitatively achieving the folding time and accurately understanding how the sequence determines the protein folding remain to be a key challenge.

In this Letter, we propose a quantum strategy to formulate protein folding as a quantum walk on a definite graph, which provides us a general scheme without artificial hypotheses. In terms of the first-passage probability, one can calculate the folding time as the mean of the first-passage time. The obtained folding time in terms of our quantum scheme is much shorter than the one obtained via classical random walks. This idea is expected to open a new avenue for investigating the protein folding theoretically, which may motivate a necessary step toward developing technology for protein engineering and designing protein-based nanodevices.[22]

Theoretical consideration: We describe the protein structure by the frequently adopted lattice model,[23–26] namely, a protein is regarded as a chain of non-own intersecting unit (usually referring an amino-acid residue) of a given length on the two-dimensional square lattice. For a protein with n amino-acid residues, we can calculate the total number N_n of distinct lattice conformations that distinguish various protein intermediate structures. For instance, we have $N_4 = 4$ and $N_6 = 22$. This provides us a set with N_n objects, and we call it the structure set and denote it by $\mathscr{S}_n = \{s_1, s_2, \cdots, s_{N_n}\}$ hereafter.

In order to study the protein folding process, we propose a concept of one-step folding. On the basis of the lattice model, we can naturally define the one-step folding by one displacement of an amino acid in one of the lattice sites. This enables us to establish certain connections between distinct points in the

*Supported by National Key R&D Program of China under Grant No 2017YFA0304304, and partially by the Fundamental Research Funds for the Central Universities.

**Corresponding author. Email: yqli@zju.edu.cn

set $\mathscr{S}_n$ and to have a connection graph $\mathscr{G}_n$. In other words, two structures can be connected via one-step folding if their conformation differs in one site only. As a conceptual illustration, we plot the structure set $\mathscr{S}_4$, the connection graphs $\mathscr{G}_4$ and $\mathscr{G}_6$ in Fig. 1 (the $\mathscr{S}_6$ in Fig. S1 in the Supplementary Material). Such a graph $\mathscr{G}_n$ is described by the so-called adjacency matrix $\mathrm{Mat}(J_{\mathrm{ab}})$ that characterizes a classical random walk[27] on the graph.

Folding as a quantum walk: Letting $|s_a\rangle$ denote the state of a protein structure in the shape of the a-th lattice conformation, we will have a quantum Hamiltonian in an N_n-dimensional Hilbert space, $\mathscr{H} = \{|s_a\rangle \mid a = 1, 2, \cdots, N_n\}$, namely,

$$\hat{H}_0 = -\sum_{a,b} J_{ab}|s_a\rangle\langle s_b|, \tag{1}$$

where J_{ab} refers to the connection between different points in the structure set, i.e., J_{ab} is nonzero only if the a-th protein structure s_a can be transited into the b-th structure s_b by a one-step folding. With these physics pictures one can also investigate quantum walk[28–30] on the aforementioned graph.

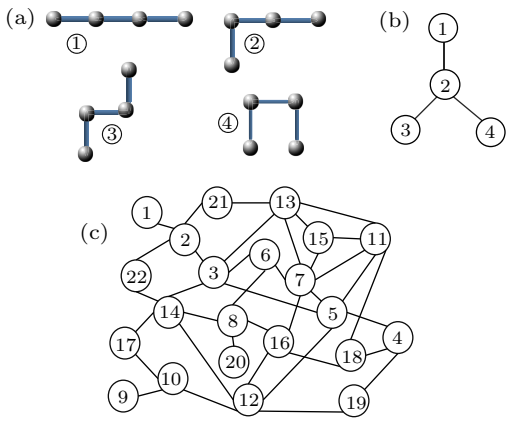

Fig. 1. Structure sets and connection graphs. (a) There are four distinct structures for the amino-acid chain with 4 residues, thus the corresponding structure set $\mathscr{S}_4$ contains 4 objects. (b) The connection graph $\mathscr{G}_4$ includes 4 vertices, which happens to be a three-star graph. (c) The connection graph $\mathscr{G}_6$ includes 22 vertices.

From the coarse grained point of view, the 20 amino acids are classified[24] into hydrophobic and hydrophilic (it is also called polar) groups according to their contact interaction. As H and P represent the hydrophobic and polar amino acids conventionally, a sequence of n amino acids can be labeled by $\boldsymbol{q} = (q_1, q_2, \cdots, q_n)$ where q_k with $k = 1, 2, \cdots, n$ refers to either H or P. Thus there will be totally a set of 2^n possible sequences. Let us call the entire of the whole random sequences the sequence set denoted by $\mathscr{Q}_n = \{[\nu] \mid \nu = 1, 2, \cdots, 2^n\}$. For any definite sequence-$[\nu]$ specified by a $\boldsymbol{q}$, we can calculate the total contact energy[25,26] for each structure in $\mathscr{S}_n$,

$$\mathcal{E}_a^{[\nu]} = \sum_{k<l} E_{q_k q_l}\delta_{|\boldsymbol{r}_k^a - \boldsymbol{r}_l^a|,1}(1 - \delta_{|k-l|,1}), \tag{2}$$

where $a = 1, 2, \cdots, N_n$ labels different structures, k and l denote the successive labels of the amino-acid residues in the sequence (i.e., the order in the chain), while $\boldsymbol{r}^a_{k(l)}$ stands for the coordinate position of the $k(l)$-th residue in the a-th structure and $q_{k(l)}$ refers to either H or P. Here the notation of Kronecker delta is adopted, i.e., $\delta_{\alpha,\beta} = 1$ if $\alpha = \beta$, and $\delta_{\alpha,\beta} = 0$ if $\alpha \neq \beta$. It is widely believed that the native structure of a protein possesses the lowest free energy.[31] This can be interpreted by the hydrophobic force that drives the protein to fold into a compact structure with hydrophobic residues inside as many as possible.[24] Thus the H-H contacts are more favorite in the lattice model,[24,32–34] which can be characterized by choosing $E_{\mathrm{PP}} = 0$, $E_{\mathrm{HP}} = -1$, and $E_{\mathrm{HH}} = -2.3$ as adopted in Ref. [25].

With the contact energy (2) for every structure, the potential term can be expressed as

$$V^{[\nu]} = \sum_a \mathcal{E}_a^{[\nu]}|s_a\rangle\langle s_a|. \tag{3}$$

Thus the total Hamiltonian for a definite sequence-$[\nu]$ is given by $\hat{H}^{[\nu]} = \hat{H}_0 + V^{[\nu]}$. Clearly, the kinetic term $\hat{H}_0$ is determined by the connection graph $\mathscr{G}_n$ merely while the potential term $V^{[\nu]}$ defined on the structure set $\mathscr{S}_n$ is related to the concrete sequence-$[\nu]$ under consideration. This means that we have a hierarchy of Hamiltonian $\{H^{[\nu]} \mid \nu = 1, 2, \cdots, 2^n\}$ actually for a theoretical study of the protein folding problem.

Note that one may obtain the same contact energy $\mathcal{E}_a$ for several different sequences. In this case, the dynamical properties are the same although those sequences may differ. Such a dynamical degeneracy implies a partition within the sequence set $\mathscr{Q}_n$. There are totally 16 possible sequences in $\mathscr{Q}_4$, which is partitioned into three subsets, i.e., $\mathscr{Q}_4 = \{Q_1, Q_2, Q_3\}$. Thus there will be three situations in the discussion on the time evolution. For $n = 6$, there are totally 64 possible sequences in $\mathscr{Q}_6$, which is partitioned into 45 subsets, i.e., $\mathscr{Q}_6 = \{Q_1, Q_2, \cdots, Q_{45}\}$ (see Tables SII & SIII in the Supplemental Material). Then a detailed discussion involves a task to solve the time evolution for the forty-five situations one by one.

Random walk with sticky vertices: As we know, the continuous time classical random walk[35] on a graph $\mathscr{G}_n$ is described by the time evolution of the probability distribution $p_a(t)$ that obeys the master equation

$$\frac{\mathrm{d}}{\mathrm{d}t}p_a(t) = \sum_b K_{ab}\, p_b(t), \tag{4}$$

where $K_{ab} = T_{\mathrm{ab}} - \delta_{ab}$ with T_{ab} being the probability-transition matrix. In the conventional classical random walk, the probability-transition matrix is determined by the adjacency matrix of an undirected graph, namely, $T_{\mathrm{ab}} = J_{\mathrm{ab}}/\deg(b)$, where $\deg(b) = \sum_c J_{\mathrm{cb}}$ represents the degree of vertex-b in the graph $\mathscr{G}_n$. However, we ought to reconsider the random walk if there are some "sticky" vertices in the graph. This

corresponds to the case that we take account of the contact energy $\mathcal{E}_a$ in the protein conformations. Thus, the probability-transition matrix should be modified so that the strength hopping into differs from that hopping out of those sticky vertices. The modified transition matrix $\tilde{T}$ is given by

$$\tilde{T}_{ab} = T_{ab} - \Gamma_{ab} + \Lambda_{\rm ab}. \tag{5}$$

Here $\Gamma_{\rm ab} = \theta(\mathcal{E}_{\rm ab})\Omega_{\rm ab}T_{\rm ab}$, $\Omega_{\rm ab} = \mathcal{E}_{\rm ab}^2/(\mathcal{E}_{\rm ab}^2+1)$, and $\Lambda_{\rm ab} = \delta_{\rm ab}\sum_c \Gamma_{\rm cb}$, in which a notation $\mathcal{E}_{\rm ab} = \mathcal{E}_a - \mathcal{E}_b$ is adopted for simplifying the expression. The expression of Ω comes from a consideration on the problem of the one-dimensional scattering by a δ-function potential well. The newly added two terms in Eq. (5) together guarantee the probability conservation. Therefore, in the presence of sticky vertices, one needs to solve the master Eq. (4) with the modified $\tilde{K} = \tilde{T} - I$ in the discussion of classical random walks.

The quantum dynamics: To accomplish a quantum mechanical understanding, we take account of the energy dissipation caused by the medium in which the folding occurs. This is governed by the Lindblad equation[36]

$$\frac{\rm d}{{\rm d}t}\hat{\rho} = \frac{1}{i\hbar}[\hat{H},\hat{\rho}] + \mathcal{L}(\hat{\rho}), \tag{6}$$

where

$$\mathcal{L}(\hat{\rho}) = \frac{\lambda}{2}\left(2L\hat{\rho}\,L^\dagger - \hat{\rho}\,L^\dagger L - L^\dagger L\hat{\rho}\right) \tag{7}$$

reflects the effect of dissipation. Here L and $L^\dagger$ are called the Lindblad operators which can be determined from the analyses of random walks in the presence of sticky vertices. The aforementioned off-diagonal part Γ in Eq. (5) provides this operator, i.e., $L^\dagger = \sum_{ab}\Gamma_{ab}|s_a\rangle\langle s_b|$. Actually, Eq. (7) presents a general expression, which becomes the traditional one in terms of Pauli matrices, $\mathcal{L}(\hat{\rho}) = (2\sigma^-\hat{\rho}\,\sigma^+ - \hat{\rho}\,\sigma^+\sigma^- - \sigma^+\sigma^-\hat{\rho})\gamma/2$ with $\gamma = \lambda\Omega^2$ for a two-level system that can be regarded as the two-vertex graph with a sticky vertex.

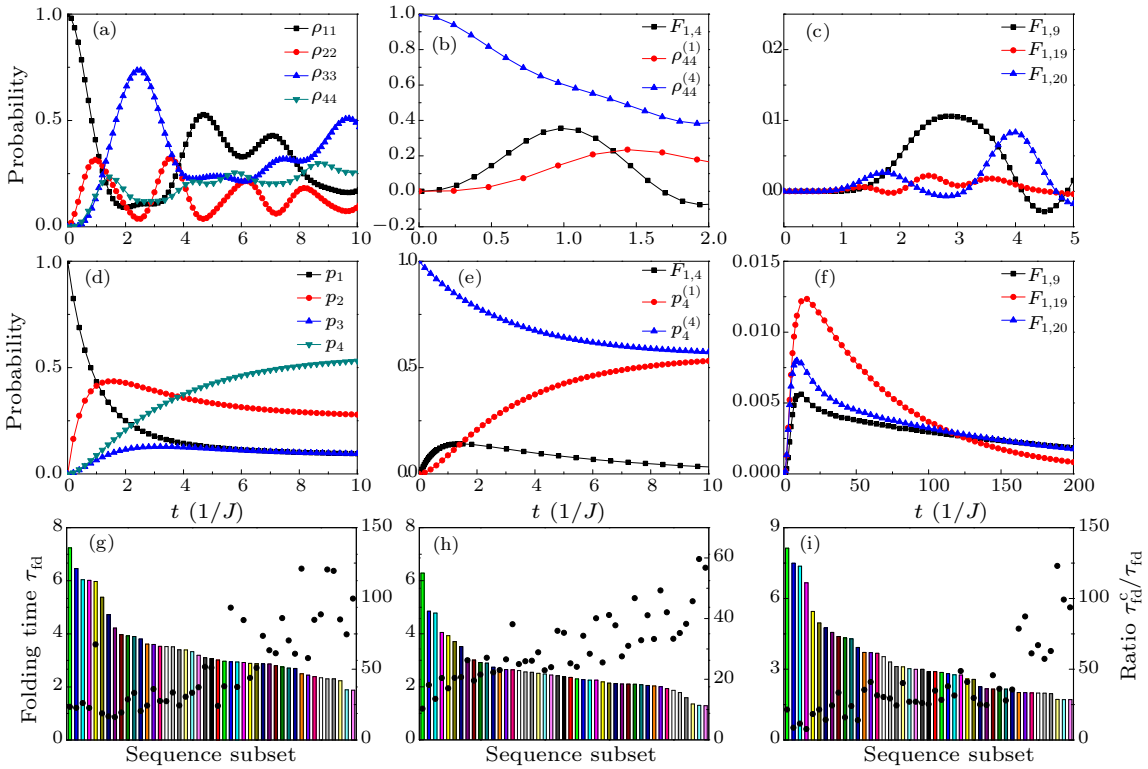

Fig. 2. Illustrations for the folding dynamics and the comparison of the folding times. (a) The time evolution of the diagonal elements of density matrix. (b) The quantum folding process for the sequence subset Q_3 with $n = 4$. It is $\rho_{44}^{(1)}$ together with $\rho_{44}^{(4)}$ that determines the first-passage probability $F_{1,4}$, which reaches zero when $t = 1.7$ and becomes negative afterwards. (c) The solved first-passage probabilities concerning the quantum folding process on the graph $\mathscr{G}_6$. $F_{1,9}$, $F_{1,19}$ and $F_{1,20}$ are the data for sequence-[37] when taking structures -9, -19 and -20 as the target states, respectively. Here $\tau_0 = 4.12$, $\tau_0 = 1.70$, and $\tau_0 = 2.44$ correspondingly. (d) The time evolution $p_1(t)$, $p_2(t)$, $p_3(t)$ and $p_4(t)$ of classical random walk on $\mathscr{G}_4$. (e) The classical folding process for subset Q_3. The solved first-passage probability is positive at finite time and approaches to zero when t goes to infinity. (f) The classical folding process on $\mathscr{G}_6$ for sequence-[37] as a comparison to the quantum case. (g)–(i) Quantum folding time $\tau_{\rm fd}$ and the ratios of classical folding time $\tau_{\rm fd}^{\rm c}$ to quantum ones. The former is plotted in terms of histogram, which is scaled by the left vertical axis, the latter is plotted by black dots, which is scaled by the right vertical axis. Correspondingly, they are the data respectively with the most compact structures s_9 (g), s_{19} (h) and s_{20} (i) as the folding targets.

We solve the density matrix $\hat{\rho}(t)$ from Eq. (6) with the initial condition $\hat{\rho}(0) = |s_1\rangle\langle s_1|$. Here $|s_1\rangle$ refers to the completely unfolded straight-line structure. To illustrate our theory intuitively, we start from the simplest model of $n = 4$, where the protein-folding problem becomes a task to investigate the quantum walk on the graph $\mathscr{G}_4$. We solve the $\hat{\rho}(t)$ numerically for the three situations Q_1, Q_2 and Q_3, respectively. In the calculation, we set $\hbar$ and J to be unity and take the time step as $\Delta t = 0.02$. Under the initial condition $\rho_{11} = 1$ while the other matrix elements vanishing when $t = 0$, we solve Eq. (6) by means of the Runge–Kutta method and obtain the magnitude of $\rho_{\rm ab}^{(1)}(t)$ at any later time, $t = j * \Delta t$ with $j = 1, 2, \cdots$. We plot the time dependence of the diagonal elements of the solved density matrix for the Q_3 case in Fig. 2(a) and the other cases in Fig. S3 in the Supplemental Material. Likewise, we solve the density matrix under another initial condition $\rho_{44}(0) = 1$ again so that the first-passage probability can be determined later on. The population of the most compact structure $|s_c\rangle$ is evaluated by the diagonal element $\rho_{\rm cc}(t)$. For instance, $c = 4$ in $\mathscr{S}_4$, and $c = 9, 19$, and 20 in $\mathscr{S}_6$. We can see that the probability of the state referring to the most compact structure $|s_4\rangle$ increases much more rapidly in the quantum folding process (Fig. 2(a)) than in the classical process (Fig. 2(d)). Toward a genuine understanding, we further study the quantum walk on the graph $\mathscr{G}_6$ by solving the density matrix numerically one by one for the aforementioned forty-five situations.

The folding time: Now we are in the position to define the protein folding time which can be formulated with the help of the concept of the mean first-passage time.[37–41] The mean first-passage time from a starting state $|s_a\rangle$ to a target state $|s_b\rangle$ is given by $\int_{t=0}^{\tau_0} tF_{a,b}(t)\mathrm{d}t \,/\, \int_{t=0}^{\tau_0} F_{a,b}(t)\mathrm{d}t$, where τ_0 represents the time period when the first-passage probability vanishes, $F_{a,b}(\tau_0) = 0$, which really occurs for the aforementioned quantum walk. For example, the solved first-passage probability $F_{1,4}(t)$ in Fig. 2(b) becomes negative after $t = 1.7$. The first-passage probability $F_{a,b}(t)$ from a state $|s_a\rangle$ to another state $|s_b\rangle$ after time t obeys the known convolution relation

$$P_{a,b}(t) = \int_0^t F_{a,b}(t')P_{b,b}(t - t')\mathrm{d}t'. \tag{8}$$

Here $P_{a,b}(t)$ denotes the probability of a state being the basis state $|b\rangle$ at time t if starting from the state $|a\rangle$ at initial time $t = 0$. Quantum mechanically, it is evaluated by the diagonal elements of the density matrix, i.e., $P_{a,b}(t) = \rho_{bb}^{(a)}(t)$, where $\rho_{bb}^{(a)}(t) = \langle b|\hat{\rho}^{(a)}(t)|b\rangle$ is solved from Eq. (6) with the initial condition $\hat{\rho}(0) = |a\rangle\langle a|$, while $P_{b,b}(t) = \rho_{bb}^{(b)}(t)$ is solved under another initial condition $\hat{\rho}(0) = |b\rangle\langle b|$. Here the superscripts are introduced to distinguish the solution from different initial conditions. In the classical case, $P_{a,b}$ and $P_{b,b}$ refer to the $p_b(t)$ solved from Eq. (4), respectively, under the initial conditions $p_c(0) = \delta_{\rm ac}$ and $p_c(0) = \delta_{\rm bc}$.

As protein folding is the process that proteins achieve their native structure, the folding time is the case that the starting state is chosen as $|s_1\rangle$ and the target states are the most compact states. For example, they are $|s_9\rangle$, $|s_{19}\rangle$ or $|s_{20}\rangle$ for $n = 6$. The formula for the calculation of the folding time is thus given by

$$\tau_{\rm fd} = \frac{\int_0^{\tau_0} tF_{1,c}(t)\mathrm{d}t}{\int_0^{\tau_0} F_{1,c}(t)\mathrm{d}t}. \tag{9}$$

To calculate the folding time we need to solve the first-passage probability $F_{1,c}(t)$ as a function of t from the convolution relation (8). As an illustration, we first consider the case of $n = 4$. For the classical folding process, we plot the $p_4^{(1)}(t)$ and $p_4^{(4)}(t)$ in Fig. 2(e). With these two time-dependent functions, the first passage-probability $F_{1,4}(t)$ can be further solved from the convolution relation (8) by numerical iterations (see Fig. 2(e)). It is nonnegative and approaches to zero when t goes to infinity. This can be understood without difficulty because the classical probability distribution changes monotonously and approaches to its steady solution at the infinite time. However, for a quantum walk the probability distribution oscillates in time. We can see that the solved density matrix shown in Fig. 2(a) and Fig. S3 of the Supplemental Material oscillates in time. With this new characteristic in quantum walk, the value of the first-passage probability solved directly from Eq. (8) appears to be negative in certain time region (see Fig. 2(b)) that is unphysical.

The zero point of $F_{1,4}(\tau_0) = 0$ determines the upper limit of the integration in the formula (9). In the simplest model with 4 residues, the classical folding times $\tau_{\rm fd}^{\rm c}$ for the sequence subsets Q_1, Q_2 and Q_3 are 6.0602, 6.0351 and 6.0180, respectively. Their corresponding quantum folding times are 1.3208, 1.2182 and 0.9670 respectively. Clearly, the quantum folding is faster than the classical folding with about four to six times even for the simplest model. In the same way, we calculate the quantum folding time for the forty-five situations for the case with 6 residues (see Tables SIV, SV & SVI in the Supplemental Material). One can see that the quantum folding is faster than the classical folding with almost ten to hundred times or more. The experimental observation[42] ever exhibited that the protein folding is much faster than the theoretical prediction based on a random conformation search process. To visualize more easily we plot the quantum folding times $\tau_{\rm fd}$ in Figs. 2(g)–2(i). For comparison, we also plot the ratios of classical folding time $\tau_{\rm fd}^{\rm c}$ to the quantum folding time $\tau_{\rm fd}$ on the same panels. In those three histograms, the longest folding time takes place for the sequence subsets Q_{13}, Q_{38} and Q_{42} while the shortest folding time occurs for the sequence subset Q_{45}, Q_{29} and Q_{29}. The largest ratios $\tau_{\rm fd}^{\rm c}/\tau_{\rm fd}$ occur for the subsets Q_{33}, Q_{31} and Q_{41} while the smallest ratios occur for Q_{17}, Q_{38} and Q_{10}.

In summary, we have proposed a self-contained general theory to investigate protein folding problem

quantum mechanically. In terms of the H–P lattice model, one can always have a structure set $\mathscr{S}_n$ for an amino-acid chain of any given number n of residues. With such a structure set, one can naturally define a connection graph $\mathscr{G}_n$ by means of our definition of one-step folding. Thus either a classical random walk or a quantum walk on the graph can be solved with standard procedures. The former implies a random conformational search while the latter involves in fact a parallel search due to the quantum mechanical coherence.[43] The application of quantum walk has attracted plenty of attention[44] to study various contemporary topics in recent years, our present strategy may open a new avenue in the area of the application of quantum walks. We have known if proteins were folded by sequentially sampling of all possible conformations, the calculated folding time would be inevitably very large because there are a very large number of degrees of freedom in an unfolded polypeptide chains. We have elucidated that the quantum evolution naturally helps us to understand a faster protein folding. In terms of the concept of first-passage probability, we can calculate the quantum protein folding time as the mean first-passage time. It is worthwhile to mention that the first-passage probability solved from the conventional convolution relation may take negative values in some time domain. This is very important for applications of the quantum approach to an investigation of protein folding time. According to our results for $n = 4$ and 6, the quantum folding time is much shorter than that obtained from classical random walk. The present theory is expected to bring in new insight features of protein folding process.

References

[1] Harrington W F and Schellman J A 1956 *C R Trav Lab Carlsberg Chim.* **30** 21
[2] Levinthal C 1968 *J. Chem. Phys.* **65** 44
[3] Mallamace F, Corsaro C, D Mallamace et al 2016 *Proc. Natl. Acad. Sci. USA* **113** 3159
[4] Portman J J, Takada S and Wolynes P G 1998 *Phys. Rev. Lett.* **81** 5237
[5] Jacksom S E 1998 *Folding Des.* **3** R81
[6] Wolynes P G, Eaton W A and Fersht A R 2012 *Proc. Natl. Acad. Sci. USA* **109** 17770
[7] Mũnoz V and Eaton W A 1999 *Proc. Natl. Acad. Sci. USA* **96** 11311
[8] Henry E R and Eqton W A 2004 *Chem. Phys.* **307** 163
[9] Englander S W and Mayne L 2017 *Proc. Natl. Acad. Sci. USA* **114** 8253
[10] Karplus M and Weaver D L 1976 *Nature* **260** 404
[11] Sali A, Shakhnovich E and Karplus M 1994 *Nature* **369** 248
[12] Guo Z Y and Thirumalai D 1995 *Biopolymers* **36** 83
[13] Fersht A R 2000 *Proc. Natl. Acad. Sci. USA* **97** 1525
[14] Oliveberg M and Wolynes P G 2005 *Q. Rev. Biophys.* **38** 245
[15] Shakhnovich E 2006 *Chem. Rev.* **106** 1559
[16] Dill K A and MacCallum J L 2012 *Science* **338** 1042
[17] Thirumalai D, Liu Z X, O'Brien E P and Reddy G 2013 *Curr. Opin. Struct. Biol.* **23** 22
[18] Piana S, Lindorff-Larsen K and Shaw D E 2012 *Proc. Natl. Acad. Sci. USA* **109** 17845
[19] Henry E R, Best R B and Eaton W A 2013 *Proc. Natl. Acad. Sci. USA* **110** 17880
[20] Snow C D, Nguyen H, Pande V and Gruebele M 2002 *Nature* **420** 102
[21] Rocklin G J et al 2017 *Science* **357** 168
[22] Mũnoz V 2014 *Proc. Natl. Acad. Sci. USA* **111** 15863
[23] Taketomi H, Ueda Y and Go N 1975 *Int. J. Peptide Protein Res.* **7** 445
[24] Dill K A 1985 *Biochemistry* **24** 1501
[25] Li H, Helling R, Tang C and Wingreen N S 1996 *Science* **273** 666
[26] Li Y Q, Ji Y Y, Mao J W and Tang X W 2005 *Phys. Rev. E* **72** 021904
[27] van Kampen N G 1997 *Stochastic Processes in Physics, Chemistry* (revised edition) (Amsterdam: North-Holland)
[28] Aharonov Y, Davidovich L and Zagury N 1993 *Phys. Rev. A* **48** 1687
[29] Farhi E and Gutmann S 1998 *Phys. Rev. A* **58** 915
[30] Manouchehri K and Wang J B 2014 *Physical Implementation of Quantum Walks* (Berlin: Springer-Verlag)
[31] Anfinsen C B 1973 *Science* **181** 223
[32] Shakhnovich E and Gutin A 1990 *J. Chem. Phys.* **93** 5967
[33] Socci N D and Onuchic J N 1994 *J. Chem. Phys.* **101** 1519
[34] Socci N D, Onuchic J N and Wolynes P G 1996 *J. Chem. Phys.* **104** 5860
[35] Montroll E W and Weiss G H 1965 *J. Math. Phys.* **6** 167
[36] Lindblad G 1976 *Commun. Math. Phys.* **48** 119
[37] Montroll E W 1969 *J. Math. Phys.* **10** 753
[38] Redner S 2001 *A Guide to First-Passage Processes* (Cambridge: Cambridge University Press)
[39] Noh J D and Rieger H 2004 *Phys. Rev. Lett.* **92** 118701
[40] Condamin S, Benichou O, Tejedor V, Voituriez R, Klafter J 2007 *Nature* **450** 77
[41] Guerin T, Levernier N, Benichou O and Voituriez R 2016 *Nature* **534** 356
[42] Duan Y and Kollman P A 1998 *Science* **282** 740
[43] Christopher C M, Christopher C P and Dutton P L 2006 *Philos. Trans. R. Soc. B* **361** 1295
[44] Xiao L et al 2017 *Nat. Phys.* **13** 1117

Supplemental Material: Quantum Approach to Fast Protein-Folding Time

Li-Hua Lu (吕丽花)[1] and You-Quan Li(李有泉)[1,2,*]

[1] *Zhejiang Province Key Laboratory of Quantum Technology & Device and Department of Physics, Zhejiang University, Hangzhou 310027, P.R. China.*

[2] *Collaborative Innovation Center of Advanced Microstructure, Nanjing University, Nanjing 210008, R.R. China.*

I. METHODS

For $n = 4$, the structure set consists of 4 objects and the connection graph defined by the one-step folding is just a three-star graph (see Fig. 1(b)). There are totally 16 possible sequences in the sequence set $\mathcal{Q}_4 = \{[1],[2],\cdots,[16]\}$ (see Table SI for details) This sequence set is partitioned into three subsets, *i.e.*, $\mathcal{Q}_4 = \{Q_1, Q_2, Q_3\}$ with $Q_1 = \{[1],[3],[5],[7]\}$, $Q_2 = \{[2],[4],[6],[8],[9],[11],[13],[15]\}$ and $Q_3 = \{[10],[12],[14],[16]\}$. Their corresponding potential energies $(\mathcal{E}_1,\mathcal{E}_2,\mathcal{E}_3,\mathcal{E}_4)$ are calculated as $(0,0,0,0)$, $(0,0,0,-1)$ and $(0,0,0,-2.3)$ respectively. Thus there will be three situations in the discussion on the time evolution. For the classical random walk on graph $\mathcal{G}_4$, we have

$$\tilde{K} = \begin{pmatrix} -1 & 1/3 & 0 & 0 \\ 1 & -1 & 1 & 1-\Omega \\ 0 & 1/3 & -1 & 0 \\ 0 & 1/3 & 0 & -1+\Omega \end{pmatrix},$$

where $\Omega = (\mathcal{E}_4)^2/\big[(\mathcal{E}_4)^2+1\big]$ with the contact energy $\mathcal{E}_4 = 0$, -1, and -2.3 respectively for Q_1, Q_2 and Q_3 cases. For each case we solve the equation (4) with the initial condition $p_a(0) = \delta_{a,1}$ and $p_a(0) = \delta_{a,4}$, respectively, and get the time evolution of $p_a^{(1)}(t)$ and $p_a^{(4)}(t)$ where the superscript is used to distinguish the solutions with different initial conditions.

A. The density matrices

The quantum walk on a graph $\mathcal{G}_n$ is described by the time evolution of a density matrix that is governed by the matrix equation (6) of the main textwhere the Hamiltonian $\hat{H}^{[\nu]}$ is of sequence $[\nu]$ dependent. As an example, we first illustrate the case of $n = 4$, for which the Hamiltonian reads

$$\hat{H}^{[\nu]} = \begin{pmatrix} 0 & -1 & 0 & 0 \\ -1 & 0 & -1 & -1 \\ 0 & -1 & 0 & 0 \\ 0 & -1 & 0 & \mathcal{E}_4^{[\nu]} \end{pmatrix}, \tag{1}$$

where $\mathcal{E}_4^{[\nu]} = 0$ for the sequences in the subset Q_1, $\mathcal{E}_4^{[\nu]} = -1$ for those in Q_2, and $\mathcal{E}_4^{[\nu]} = -2.3$ for those in Q_3. For each case, we substitute Eq. (1) into Eq. (6) of the main text to determine the time evolution of the 4 by 4 density matrix $\hat{\rho}(t) = \{\rho_{a,b}(t) \mid a,b = 1,2,3,4\}$. In our numerical calculation, we set $\hbar$ and J to be unity and take the time step as $\Delta t = 0.02$. For the initial condition, $\rho_{11}(0) = 1$ and the other matrix elements vanish when $t = 0$, we solve the aforementioned first-order differential equation (6) of the main text by means of Runge-Kutta method and obtain the magnitudes of $\rho_{ab}^{(1)}(t)$ at any later time, $t = j * \Delta t$ with $j = 1,2,\cdots$.

In order to have an intuitive picture we plot in Fig. S2 the density matrix at a certain time t when $\rho_{4,4}^{(1)}(t)$ first reaches its maximum value. The off-diagonal elements of density matrix in quantum mechanics are usually complex numbers, so we use histogram heights to evaluate the modules and colors to label the phases of the complex numbers. The time dependence of the diagonal element of the solved density matrix for the Q_3 case is plotted in Fig. 2 for an intuitive illustration. Likewise, we need to solve the density matrix for another initial condition, $\rho_{44}(0) = 1$ again so that the first-passage probability can be determined.

Similarly, the study of the quantum walk on the graph $\mathcal{G}_6$ is a task to solve the 22 by 22 density matrix from Eq. (6) of the main text for the forty-five situations (see Table SIII) one by one. Here the potential term in the total Hamiltonian is expressed as $V = \sum_{a=1}^{22} \mathcal{E}_a \mid a\rangle\langle a \mid$ with $\mathcal{E}_a \neq 0$ for $a = 4,8,9,10,16,17,18,19$ and 20 while $\mathcal{E}_a = 0$ for $a = 1,2,3,5,6,7,11,12,13,14,15,21$ and 22. In terms the solved density matrices we can calculate the fist-passage probability furthermore.

B. The first-passage probabilities

For numerical calculation, the discrete version of Eq. (8) is given by

$$F_{14}(k*\Delta t) = \frac{P_{1,4}(k*\Delta t)}{\Delta t} - \sum_{l=0}^{k-1} F_{1,4}\big(l*\Delta t\big)P_{4,4}\big((k-l)*\Delta t\big), \tag{2}$$

with $k = 1,2,\cdots$. As we have $P_{1,4}(i*\Delta t) = \rho_{44}^{(1)}(i*\Delta t)$, $P_{4,4}(i*\Delta t) = \rho_{44}^{(4)}(i*\Delta t)$ together with the natural initial conditions $F_{1,4}(0) = 0$, $P_{1,4}(0) = 0$ and $P_{4,4}(0) = 1$, the above relation (2) for $k = 1$ gives rise to $F_{1,4}(\Delta t) = P_{1,4}(\Delta t)/\Delta t$, and furthermore for $k = 2,\cdots$ iteratively gives rise to $F_{1,4}(k*\Delta t)$. Since $F_{1,4}(k*\Delta t)$ oscillates with time, when $F_{1,4}(k*\Delta t)$ first appears to be negative

* email: yqli@zju.edu.cn

value, we record the corresponding value of k as k_0. This implies that the upper limit of integration τ_0 in Eq. (9) of the main text is between the value of $(k_0-1)*\Delta t$ and $k_0*\Delta t$. In our calculation of the folding time, we take $\tau_0 \approx (k_0-1)*\Delta t$ in the discrete version of the formula (9) consequently,

$$\tau_{\rm fd} = \frac{\sum_{k=1}^{k_0-1} k*\Delta t * F_{1,4}(k*\Delta t)*\Delta t}{\sum_{k=1}^{k_0-1} F_{1,4}(k*\Delta t)*\Delta t}. \qquad (3)$$

We calculated the folding times numerically for each case, our results are listed in the Tables SIV, SV and SVI.

II. SUPPLEMENTAL FIGURES AND TABLES

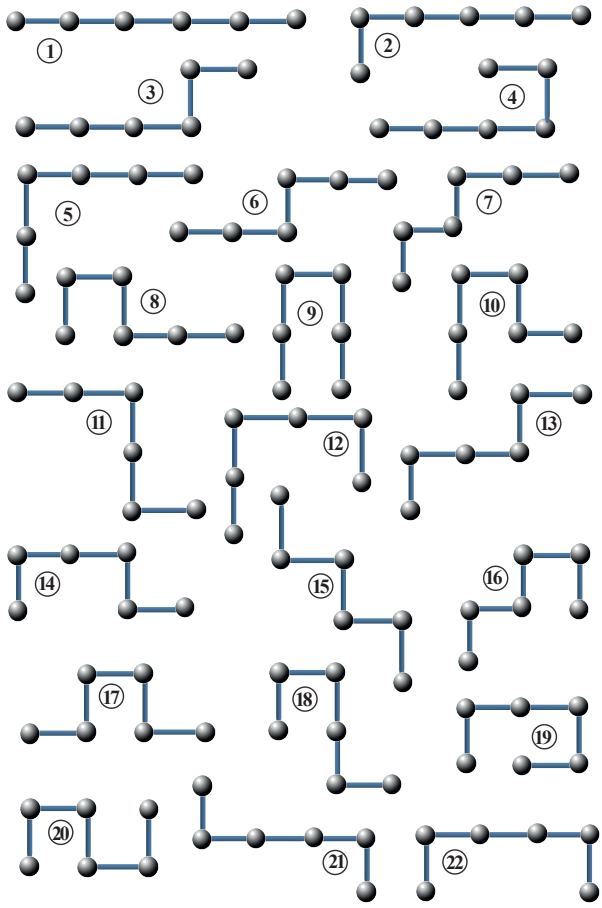

FIG. S1. The contents of the structure set $\mathcal{S}_6$. There are twenty-two distinct structures for the amino-acid chain with six residues (the case of n=6). Here the structures numbered as 9, as 19, and as 20 are called the most compact structures. The contact energy $\mathcal{E}_a \neq 0$ for the structure-a with $a = 4, 8, 9, 10, 16, 17, 18, 19$ and 20, while $\mathcal{E}_a = 0$ for the other structures.

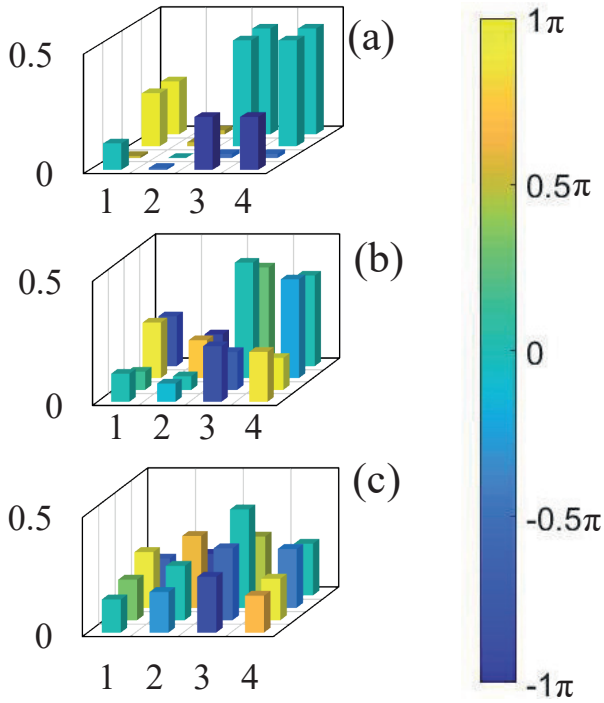

FIG. S2. Color histogram of the density matrix. The solved density matrix at the first time when $\rho_{44}^{(1)}$ reaches its maximum value is plotted in terms of colored histogram, in which the heights evaluate the modules of the matrix element and the colors measured in the color-bar present their complex-number phases. We plotted density matrices, respectively from the solutions, (a) for the subset Q_1 at $t = 1.82$, (b) for Q_2 at $t = 1.70$ and (c) for Q_3 at $t = 1.52$. Clearly, the existence of off-diagonal elements reflects the quantum coherence that speeds up the protein folding process.

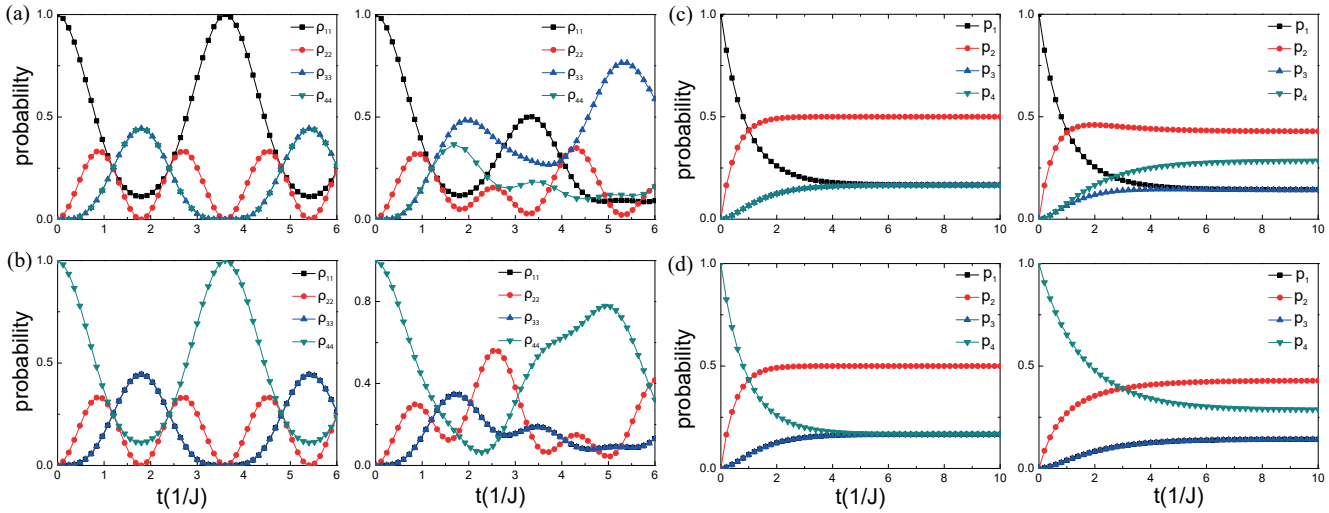

FIG. S3. The evolution of quantum and classical probabilities. The time dependence of the diagonal elements of the quantum mechanical density matrix and the corresponding classical counterparts for the other two sequence subsets Q_1 (left panel) and Q_2 (right panel). The diagonal elements of the density matrix solved from the initial conditions (a) $\rho(0) =\mid s_1\rangle\langle s_1 \mid$ and (b) $\rho(0) =\mid s_4\rangle\langle s_4 \mid$. The corresponding classical solutions of the probability distribution solved from two initial conditions (c) $p_b(0) = \delta_{b1}$ and (d) $p_b(0) = \delta_{b4}$.

TABLE SI. The collection of sequences in the sequence set Ω_4

$[1] = (P, P, P, P)$	$[2] = (P, P, P, H)$	$[3] = (P, P, H, P)$	$[4] = (P, P, H, H)$
$[5] = (P, H, P, P)$	$[6] = (P, H, P, H)$	$[7] = (P, H, H, P)$	$[8] = (P, H, H, H)$
$[9] = (H, P, P, P)$	$[10] = (H, P, P, H)$	$[11] = (H, P, H, P)$	$[12] = (H, P, H, H)$
$[13] = (H, H, P, P)$	$[14] = (H, H, P, H)$	$[15] = (H, H, H, P)$	$[16] = (H, H, H, H)$

TABLE SII. The collection of sequences in the sequence set $\mathcal{Q}_6$

$[1]=(P,P,P,P,P,P)$	$[2]=(P,P,P,P,P,H)$	$[3]=(P,P,P,P,H,P)$
$[4]=(P,P,P,P,H,H)$	$[5]=(P,P,P,H,P,P)$	$[6]=(P,P,P,H,P,H)$
$[7]=(P,P,P,H,H,P)$	$[8]=(P,P,P,H,H,H)$	$[9]=(P,P,H,P,P,P)$
$[10]=(P,P,H,P,P,H)$	$[11]=(P,P,H,P,H,P)$	$[12]=(P,P,H,P,H,H)$
$[13]=(P,P,H,H,P,P)$	$[14]=(P,P,H,H,P,H)$	$[15]=(P,P,H,H,H,P)$
$[16]=(P,P,H,H,H,H)$	$[17]=(P,H,P,P,P,P)$	$[18]=(P,H,P,P,P,H)$
$[19]=(P,H,P,P,H,P)$	$[20]=(P,H,P,P,H,H)$	$[21]=(P,H,P,H,P,P)$
$[22]=(P,H,P,H,P,H)$	$[23]=(P,H,P,H,H,P)$	$[24]=(P,H,P,H,H,H)$
$[25]=(P,H,H,P,P,P)$	$[26]=(P,H,H,P,P,H)$	$[27]=(P,H,H,P,H,P)$
$[28]=(P,H,H,P,H,H)$	$[29]=(P,H,H,H,P,P)$	$[30]=(P,H,H,H,P,H)$
$[31]=(P,H,H,H,H,P)$	$[32]=(P,H,H,H,H,H)$	$[33]=(H,P,P,P,P,P)$
$[34]=(H,P,P,P,P,H)$	$[35]=(H,P,P,P,H,P)$	$[36]=(H,P,P,P,H,H)$
$[37]=(H,P,P,H,P,P)$	$[38]=(H,P,P,H,P,H)$	$[39]=(H,P,P,H,H,P)$
$[40]=(H,P,P,H,H,H)$	$[41]=(H,P,H,P,P,P)$	$[42]=(H,P,H,P,P,H)$
$[43]=(H,P,H,P,H,P)$	$[44]=(H,P,H,P,H,H)$	$[45]=(H,P,H,H,P,P)$
$[46]=(H,P,H,H,P,H)$	$[47]=(H,P,H,H,H,P)$	$[48]=(H,P,H,H,H,H)$
$[49]=(H,H,P,P,P,P)$	$[50]=(H,H,P,P,P,H)$	$[51]=(H,H,P,P,H,P)$
$[52]=(H,H,P,P,H,H)$	$[53]=(H,H,P,H,P,P)$	$[54]=(H,H,P,H,P,H)$
$[55]=(H,H,P,H,H,P)$	$[56]=(H,H,P,H,H,H)$	$[57]=(H,H,H,P,P,P)$
$[58]=(H,H,H,P,P,H)$	$[59]=(H,H,H,P,H,P)$	$[60]=(H,H,H,P,H,H)$
$[61]=(H,H,H,H,P,P)$	$[62]=(H,H,H,H,P,H)$	$[63]=(H,H,H,H,H,P)$
$[64]=(H,H,H,H,H,H)$		,

TABLE SIII. The degeneracy of contact energies in $\mathcal{G}_6$

Q_1={$[1]$}	Q_2={$[2]$}	Q_3={$[3],[17]$}
Q_4={$[4],[18]$}	Q_5={$[5]$}	Q_6={$[6],[41]$}
Q_7={$[7],[21]$}	Q_8={$[8],[22],[43],[57]$}	Q_9={$[9]$}
Q_{10}={$[10]$}	Q_{11}={$[11],[25]$}	Q_{12}={$[12],[26]$}
Q_{13}={$[13]$}	Q_{14}={$[14]$}	Q_{15}={$[15],[29]$}
Q_{16}={$[16],[30]$}	Q_{17}={$[19]$}	Q_{18}={$[20]$}
Q_{19}={$[23]$}	Q_{20}={$[24],[59]$}	Q_{21}={$[27]$}
Q_{22}={$[28]$}	Q_{23}={$[31]$}	Q_{24}={$[32]$}
Q_{25}={$[33]$}	Q_{26}={$[34]$}	Q_{27}={$[35],[49]$}
Q_{28}={$[36],[50]$}	Q_{29}={$[37]$}	Q_{30}={$[38]$}
Q_{31}={$[39],[53]$}	Q_{32}={$[40],[54]$}	Q_{33}={$[42]$}
Q_{34}={$[44],[58]$}	Q_{35}={$[45]$}	Q_{36}={$[46]$}
Q_{37}={$[47],[61]$}	Q_{38}={$[48],[62]$}	Q_{39}={$[51]$}
Q_{40}={$[52]$}	Q_{41}={$[55]$}	Q_{42}={$[56]$}
Q_{43}={$[60]$}	Q_{44}={$[63]$}	Q_{45}={$[64]$}

The set $\mathcal{G}_6$ is partitioned into forty-five subsets within which all sequences possess the same energies.

TABLE SIV. Comparison of the protein folding times for the forty-five situations (A)

subset	$\tau_{\rm fd}$	$\tau_{\rm fd}^{\rm c}$	$\tau_{\rm fd}/\tau_{\rm fd}^{\rm c}$	subset	$\tau_{\rm fd}$	$\tau_{\rm fd}^{\rm c}$	$\tau_{\rm fd}/\tau_{\rm fd}^{\rm c}$
Q_1 :	6.013334	136.035087	22.622240	Q_2 :	3.098551	160.247563	51.716936
Q_3 :	3.520525	96.315062	27.358153	Q_4 :	2.967067	112.623345	37.957803
Q_5 :	6.458355	146.705338	22.715589	Q_6 :	2.866759	181.768820	63.405686
Q_7 :	3.392589	103.502335	30.508362	Q_8 :	2.889039	126.895859	43.923207
Q_9 :	6.038505	157.593573	26.098111	Q_{10} :	2.921799	247.545879	84.723788
Q_{11} :	3.327806	110.875024	33.317755	Q_{12} :	2.801380	171.669173	61.280217
Q_{13} :	7.234799	169.607081	23.443233	Q_{14} :	2.946329	275.445274	93.487616
Q_{15} :	3.191671	118.864775	37.242177	Q_{16} :	2.708122	190.313983	70.275262
Q_{17} :	4.216321	68.078909	16.146519	Q_{18} :	4.724344	78.765355	16.672231
Q_{19} :	3.016037	72.794175	24.135704	Q_{20} :	3.612531	87.963045	24.349423
Q_{21} :	3.804250	77.658548	20.413629	Q_{22} :	3.512217	117.651074	33.497667
Q_{23} :	3.396357	82.796081	24.377909	Q_{24} :	3.900503	129.733781	33.260782
Q_{25} :	3.066039	156.489675	51.039688	Q_{26} :	2.388859	202.780028	84.885725
Q_{27} :	2.937746	110.044318	37.458759	Q_{28} :	2.441537	141.135648	57.806066
Q_{29} :	2.869247	210.959777	73.524439	Q_{30} :	2.303083	275.098917	119.448112
Q_{31} :	2.873812	146.665698	51.035244	Q_{32} :	2.232110	189.940402	85.094553
Q_{33} :	2.494938	301.894318	121.002734	Q_{34} :	2.343357	208.004786	88.763593
Q_{35} :	2.752986	237.048877	86.106096	Q_{36} :	5.974401	403.400204	67.521448
Q_{37} :	2.697952	164.314142	60.903286	Q_{38} :	2.304499	277.603821	120.461680
Q_{39} :	3.968589	77.036636	19.411593	Q_{40} :	3.528882	97.314095	27.576466
Q_{41} :	5.378916	100.994382	18.775973	Q_{42} :	3.597822	129.316623	35.943030
Q_{43} :	1.893287	141.255927	74.608830	Q_{44} :	3.922487	112.584764	28.702393
Q_{45} :	1.877747	187.603586	99.908873				

The data in the above is calculated by taking the structure-9 as the target state.

TABLE SV. Comparison of the protein folding times for the forty-five situations (B)

subset	$\tau_{\rm fd}$	$\tau_{\rm fd}^{\rm c}$	$\tau_{\rm fd}/\tau_{\rm fd}^{\rm c}$	subset	$\tau_{\rm fd}$	$\tau_{\rm fd}^{\rm c}$	$\tau_{\rm fd}/\tau_{\rm fd}^{\rm c}$
Q_1 :	3.007868	58.811334	19.552498	Q_2 :	2.479394	56.885456	22.943290
Q_3 :	2.915515	62.760625	21.526428	Q_4 :	2.737002	60.829525	22.224874
Q_5 :	2.662492	61.269774	23.012191	Q_6 :	2.184729	55.766683	25.525675
Q_7 :	2.610164	65.195489	24.977545	Q_8 :	2.355810	59.440630	25.231504
Q_9 :	2.561153	66.410402	25.929885	Q_{10} :	2.121793	80.139792	37.769845
Q_{11} :	2.650392	70.320819	26.532233	Q_{12} :	2.376243	83.876242	35.297839
Q_{13} :	2.298248	55.371229	24.092800	Q_{14} :	1.866984	62.231172	33.332461
Q_{15} :	2.443572	58.510481	23.944652	Q_{16} :	2.099786	65.095912	31.001213
Q_{17} :	3.058518	80.326256	26.263130	Q_{18} :	2.892302	78.325642	27.080727
Q_{19} :	4.049810	82.688870	20.417963	Q_{20} :	3.704805	75.757923	20.448559
Q_{21} :	4.850417	87.771468	18.095654	Q_{22} :	2.640431	100.666945	38.125194
Q_{23} :	2.511114	72.516173	28.878089	Q_{24} :	2.270134	77.941553	34.333459
Q_{25} :	1.352143	61.804911	45.708857	Q_{26} :	2.105304	57.913441	27.508351
Q_{27} :	2.544296	66.400618	26.097835	Q_{28} :	2.252789	63.908920	28.368800
Q_{29} :	1.286258	73.047173	56.790452	Q_{30} :	3.928691	66.756540	16.992057
Q_{31} :	1.301468	77.602514	59.626909	Q_{32} :	3.513602	72.667062	20.681643
Q_{33} :	1.785740	62.875193	35.209601	Q_{34} :	2.030462	67.511972	33.249562
Q_{35} :	4.781740	64.586440	13.506891	Q_{36} :	1.588760	60.753000	38.239256
Q_{37} :	2.076350	68.193510	32.842974	Q_{38} :	6.287673	64.546238	10.265521
Q_{39} :	2.414371	86.787849	35.946360	Q_{40} :	2.252013	90.261891	40.080537
Q_{41} :	2.096400	97.939811	46.718093	Q_{42} :	2.004589	98.749514	49.261726
Q_{43} :	2.138715	88.018182	41.154704	Q_{44} :	2.051656	84.318310	41.097684
Q_{45} :	1.935271	81.391188	42.056739				

The data in the above is calculated by taking the structure-19 as the target state.

TABLE SVI. Comparison of the protein folding times for the forty-five situations (C)

subset	$\tau_{\rm fd}$	$\tau^{\rm c}_{\rm fd}$	$\tau_{\rm fd}/\tau^{\rm c}_{\rm fd}$	subset	$\tau_{\rm fd}$	$\tau_{\rm fd}$	$\tau_{\rm fd}/\tau^{\rm c}_{\rm fd}$
Q_1 :	3.534390	107.326690	30.366397	Q_2 :	3.109753	75.781759	24.369061
Q_3 :	3.676584	115.724340	31.476050	Q_4 :	3.021071	81.647239	27.025925
Q_5 :	1.985434	113.879920	57.357696	Q_6 :	2.996953	81.103898	27.062119
Q_7 :	1.998518	122.248609	61.169631	Q_8 :	2.765095	86.798091	31.390636
Q_9 :	2.896183	73.311216	25.313047	Q_{10} :	6.663490	51.723617	7.762241
Q_{11} :	2.996405	78.338356	26.144115	Q_{12} :	3.925446	54.768113	13.952074
Q_{13} :	2.570879	76.241005	29.655618	Q_{14} :	2.167717	53.557491	24.706865
Q_{15} :	2.865303	81.211569	28.343100	Q_{16} :	2.252009	56.512998	25.094481
Q_{17} :	3.702682	151.733536	40.979359	Q_{18} :	4.962379	106.785040	21.518921
Q_{19} :	2.010765	158.129502	78.641463	Q_{20} :	4.560383	111.178045	24.379103
Q_{21} :	5.453139	99.879543	18.315972	Q_{22} :	4.751003	67.798839	14.270426
Q_{23} :	4.285138	102.503862	23.920784	Q_{24} :	4.327710	69.153246	15.979177
Q_{25} :	1.966476	123.623213	62.865356	Q_{26} :	3.305973	96.940512	29.322838
Q_{27} :	1.992959	133.386930	66.929089	Q_{28} :	2.592900	106.332739	41.009194
Q_{29} :	1.710127	160.168363	93.658753	Q_{30} :	3.101977	124.796863	40.231395
Q_{31} :	1.713752	169.914771	99.147818	Q_{32} :	2.756688	134.294122	48.715749
Q_{33} :	2.157100	60.285284	27.947376	Q_{34} :	7.491422	65.002142	8.676876
Q_{35} :	2.896166	100.987316	34.869312	Q_{36} :	2.057256	73.265667	35.613296
Q_{37} :	2.814767	106.795670	37.941211	Q_{38} :	2.157124	78.093837	36.202757
Q_{39} :	2.008037	175.248216	87.273400	Q_{40} :	4.387504	146.585522	33.409775
Q_{41} :	1.721760	211.679379	122.943604	Q_{42} :	8.130396	174.980161	21.521727
Q_{43} :	7.367946	85.202543	11.563948	Q_{44} :	3.710836	131.651748	35.477652
Q_{45} :	2.161168	98.745327	45.690722				

The data in the above is calculated by taking the structure-20 as the target state.

TABLE SVII. Table of notations

n	number of the amino-acid residues
N_n	total number of protein structure (the lattice conformation)
$\mathcal{S}_n$	the structure set
$\mathcal{G}_n$	the connection graph
Ω_n	the sequence set
a, b, c	index labelling the specific structure, which takes from 1 to N_n
$\mathcal{E}_a^{[\nu]}$	contact energy of the structure s_a, the superscript refers a given sequence $[\nu]$
$\mathcal{E}_{ab}$	the energy difference $\mathcal{E}_{ab} = \mathcal{E}_a - \mathcal{E}_b$
J_{ab}	the elements of adjacency matrix that characterizes the graph $\mathcal{G}_n$
T_{ab}	the elements of the probability transition matrix, $T_{ab} = J_{ab}/\deg(b)$
$\deg(b)$	the degree of vertex-b, $\deg(b) = \sum_a J_{ab}$
L, $L^\dagger$	the Lindblad operator
$[\nu]$	labels for a particular sequence, where ν takes from 1 to 2^n
Q_1, Q_2, etc.	subsets in Ω_n, the contact energies in each subset are degenerate
$\hat{\rho}$	density matrix
ρ_{ab}	the matrix elements of $\hat{\rho}$
p_a	classical probability distributions
$p^{(1)}(t)$, $\hat{\rho}^{(1)}(t)$	the superscript here specifies the initial condition from which the solution is obtained
$P_{a,b}(t)$	probability from structure-a to structure-b at time t
$F_{a,b}(t)$	the first-passage probability from structure-a to structure-b at time t
τ_0	the time period that the first-passage probability vanishes $F_{a,b}(\tau_0) = 0$
$\tau_{\rm fd}$	quantum folding time
$\tau_{\rm fd}^{\rm c}$	classical folding time